Buoyancy flux, turbulence, and the gas transfer coefficient in a stratified lake

Sally MacIntyre,[1,2] Anders Jonsson,[3] Mats Jansson,[3] Jan Aberg,[3] Damon E. Turney,[2] and Scott D. Miller[4]

Received 1 June 2010; revised 14 October 2010; accepted 19 October 2010; published 22 December 2010.

[1] Gas fluxes from lakes and other stratified water bodies, computed using conservative values of the gas transfer coefficient k_{600}, have been shown to be a significant component of the carbon cycle. We present a mechanistic analysis of the dominant physical processes modifying k_{600} in a stratified lake and resulting new models of k_{600} whose use will enable improved computation of carbon fluxes. Using eddy covariance results, we demonstrate that i) higher values of k_{600} occur during low to moderate winds with surface cooling than with surface heating; ii) under overnight low wind conditions k_{600} depends on buoyancy flux β rather than wind speed; iii) the meteorological conditions at the time of measurement and the inertia within the lake determine k_{600}; and iv) eddy covariance estimates of k_{600} compare well with predictions of k_{600} using a surface renewal model based on wind speed and β. **Citation:** MacIntyre, S., A. Jonsson, M. Jansson, J. Aberg, D. E. Turney, and S. D. Miller (2010), Buoyancy flux, turbulence, and the gas transfer coefficient in a stratified lake, *Geophys. Res. Lett.*, *37*, L24604, doi:10.1029/2010GL044164.

1. Introduction

[2] Lakes and reservoirs are sources of climatically-active gases to the atmosphere and are a significant component of the global carbon budget [*Cole et al.*, 2007]. Consequently, it is of critical importance that carbon fluxes from lakes be accurately estimated. Computations of carbon fluxes from lakes most often rely on gas transfer coefficients (k_{600}) and in most cases use conservative values of k_{600} or wind-based equations [*Cole and Caraco*, 1998]. The gas transfer coefficient k_{600}, however, depends upon the turbulence at the air-water interface [*Banerjee and MacIntyre*, 2004; *McGillis et al.*, 2004] which does not depend upon wind alone. For instance, the turbulence from heat loss that occurs when buoyancy fluxes (β) are negative often exceeds that from wind mixing in tropical lakes and is the dominant cause of mixing in many small lakes world-wide [*MacIntyre et al.*, 2002; *MacIntyre and Melack*, 2009]. Stratification, which acts to suppress turbulence, is associated with a positive β, and is not considered in wind-based models. The surface renewal model, which can be formulated as $k_{600} = c_1 (\varepsilon\nu)^{0.25}$ is an alternate approach to wind-based models as it explicitly takes into account the suite of processes which influence turbulence near the air-water interface [*Soloviev and Schluessel*, 1994; *MacIntyre et al.*, 1995, 2001; *Zappa et al.*, 2007; *Turney and Banerjee*, 2008]. In this model, ε is the rate of dissipation of turbulent kinetic energy in the water near the interface and characterizes the turbulence, ν is the kinematic viscosity, and c_1 is an empirically derived, depth dependent coefficient. Despite its potential to accurately quantify the physical processes causing gas flux, and despite the importance of lakes in carbon budgets [*Cole et al.*, 2007], the surface renewal model has rarely been applied to describe gas flux in lakes [*Crill et al.*, 1988; *Vachon et al.*, 2010].

[3] Estimating gas flux with the eddy covariance technique (EC) (reviewed by *Wanninkhof et al.* [2009]), for which averages are obtained over 30 minute intervals, allows computation of k_{600} on the time scale of changes in meteorological forcing, thermal structure of the surface layer of lakes and oceans, and turbulence at the air-water interface. The gas transfer coefficient k is computed as $k = F_c / (C_w - \alpha C_a)$ where F_c is flux in moles per unit area per unit time, C_w and C_a are the concentrations of gas across the air-water interface, and α is the Ostwald solubility coefficient; k is normalized to correspond to CO_2 at 20°C and denoted as k_{600}. The relative role of different physical processes in producing or damping turbulence can be assessed by comparing k_{600} derived from eddy covariance measurements (k_{600EC}) with k_{600} computed from estimates of ε under different meteorological conditions. Models of k_{600} that take into account this variability can be developed as needed for improved estimates of gas flux.

[4] The time series measurements of meteorology, water temperature, and k_{600EC} from EC measurements [*Jonsson et al.*, 2008; *Aberg et al.*, 2010] are reanalyzed here in the context of turbulence production at the air-water interface to develop models of k_{600}. We compute ε using the empirical model of *Lombardo and Gregg* [1989], k_{600} using the surface renewal model, and compare the modeled estimates with those obtained from eddy covariance to evaluate the processes determining k_{600} and the applicability of the surface renewal model. We develop regressions for k_{600} as a function of wind speed for $\beta > 0$ and $\beta < 0$.

2. Methods

[5] Measurements from Lake Meräsjarvi, Sweden (67°33′00″N, 21°58′30″E; surface area 3.8 km^2) from 2 July to 3 are

[1]Department of Ecology, Evolution and Marine Biology, University of California, Santa Barbara, California, USA.
[2]Earth Research Institute, University of California, Santa Barbara, California, USA.
[3]Department of Ecology and Environmental Sciences, Umea University, Umea, Sweden.
[4]Atmospheric Sciences Research Center, State University of New York at Albany, Albany, New York, USA.

0094-8276/10/2010GL044164

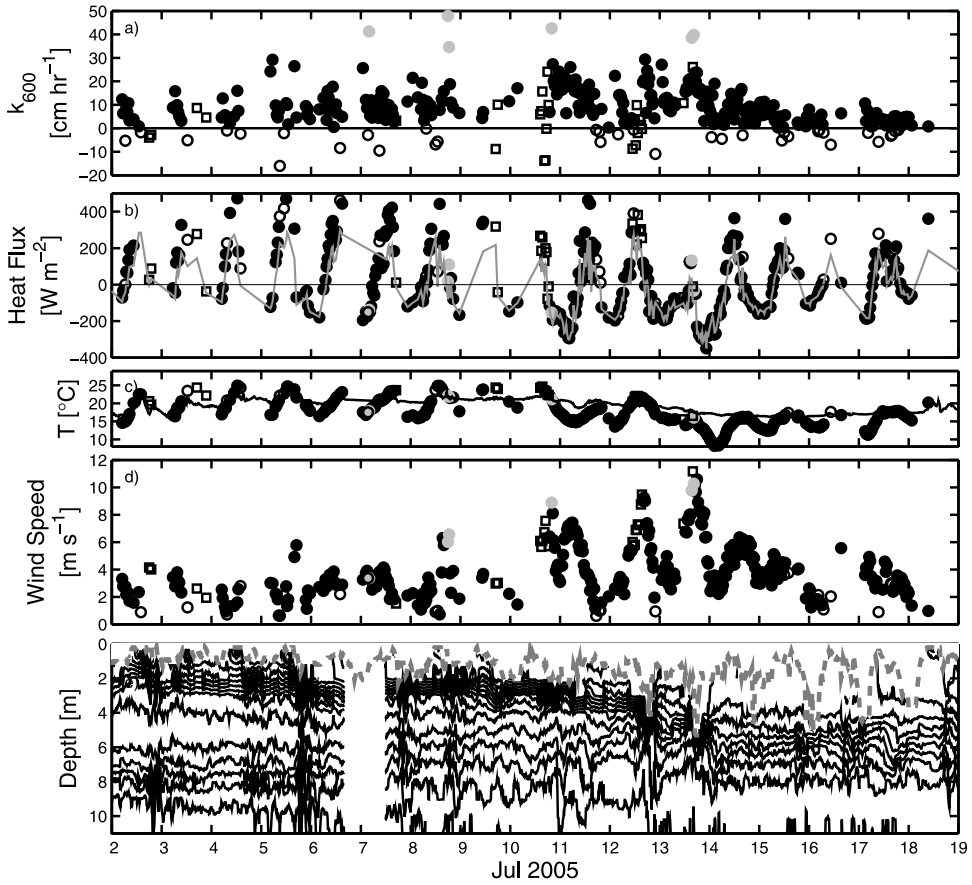

Figure 1. Time series measurements from 2–19 July 2005 of (a) k_{600} from eddy covariance measurements k_{600EC}, (b) total heat flux (dots) and effective heat flux (gray line), (c) air (dots) and surface water temperatures (line), (d) U_{10} (dots), (e) mixing depth z_{AML} (dashed gray line), isotherms (black lines) at 1°C intervals and with 8°C contour in lower left. Data at times when $k_{600EC} < 0$ (open circles), when k_{600EC} exceeded 30 cm hr^{-1} (gray circles), and examples when analysis suggested the footprint may have exceeded the distance from the measurement station to land (not used, open boxes).

used in this reanalysis (Figure 1). Following *Imberger* [1985] and *MacIntyre et al.* [2002, 2009], we compute the depth of the actively mixing layer (z_{AML}); effective heat flux; buoyancy flux β; water side Monin-Obukhov length scale divided by mixed layer depth (L_w/z_{AML}); and buoyancy frequency (N). Temperature was measured with thermocouples (accuracy of 0.2°C) at 0.5 m intervals in the upper three meters and thermistors (accuracy of 0.5°C) at ~1 m intervals from the surface to the bottom. In defining z_{AML}, the requisite step change in temperature from the surface temperature is set equivalent to the accuracy of the loggers. Values of net short wave radiation, visible radiation (~400 nm to 700 nm), net long wave radiation, and the diffuse attenuation coefficient (k_d = 0.22 m^{-1}) are necessary to calculate effective heat flux and β. To estimate net short wave radiation from the net radiation measurements by *Jonsson et al.* [2008], we approximate net long wave radiation as −50 W m^{-2} based on typical values for arctic lakes [*MacIntyre et al.*, 2009] and add it to net radiation. Downwelling visible radiation is then estimated as 43% of net short wave radiation. The measured wind speeds (measurements initially at 2.6 m but primarily at 1.6 m) were corrected to 10 m height following *Jonsson et al.* [2008]. Following the logic of *Jonsson et al.* [2008] we use all values of k_{600} < 40 cm hr^{-1} in this analysis. The atmosphere was neutral or slightly unstable for much of the study period, Monin-Obukhov length scale L < = 0 (data not shown). We rejected values of k_{600} when L > 0 as we suspected a footprint problem at those times.

[6] Dissipation rates, ε were computed from β and the water friction velocity u_{*w} following *Lombardo and Gregg* [1989]. $\varepsilon = 0.84(0.58\beta + 1.76u^3_{*w}/kz)$ where the coefficients were determined empirically; k is the von Karman constant and z is depth. u_{*w} is computed from shear stress at the air-water interface assuming it is equal on either side of the interface, giving $\tau_w = \rho_w u^2_{*w} = \tau_a = \rho_a u^2_{*a}$ where τ_a and τ_w are shear stress on air and water side of the air-water interface; u_{*a} is the air friction velocity computed from measured wind speeds following *MacIntyre et al.* [2002]; and ρ_a and ρ_w are density of air and water respectively. Following *Imberger* [1985] we let $z = z_{AML}$. Computation of ε with β instead of w_*, the velocity scale for convection, as by *Imberger* [1985], allows a portion of the turbulence to be damped when heating occurs. The gas transfer coefficient from these dissipation estimates using the surface renewal model was computed as $k_{600SR} = c_1(\varepsilon\,\nu)^{1/4}$ with c_1 = 1.2.

3. Results

3.1. Meteorology, k_{600}, and Lake Thermal Structure

[7] The magnitude of the gas transfer coefficients varied over diel cycles as winds varied and as the lake heated and

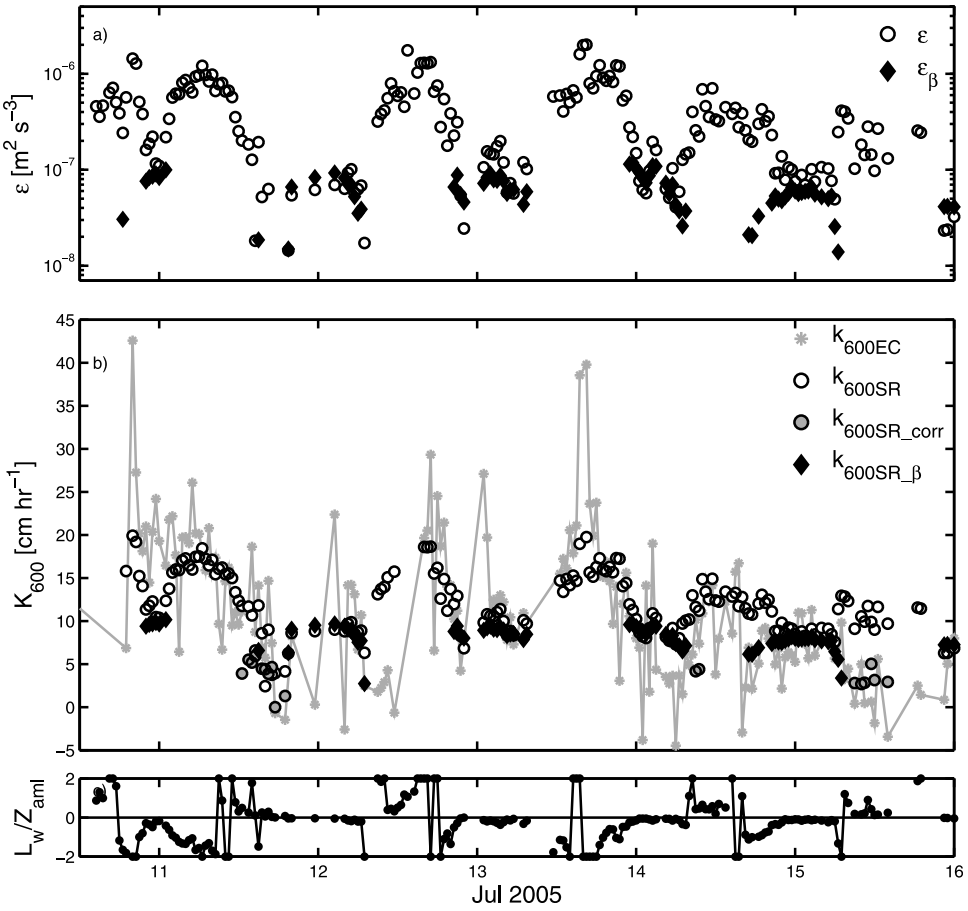

Figure 2. Time series from 10 to 16 July of (a) rate of dissipation of turbulent kinetic energy ε (open circles) and dissipation from β, ε_β, computed when $L_w/z_{AML} < 0$ and measured winds < 4 m s^{-1} (diamonds) and (b) k_{600EC} (gray); and k_{600} from the surface renewal model k_{600SR} (open circles); k_{600SR} computed from ε_β, k_{600SR_β} (diamonds); and k_{600SR} corrected for heating and water column stratification when $L_w/z_{AML} > 0$ and measured winds < 3 m s^{-1} (gray circles); and (c) L_w/z_{AML} with $L_w/z_{AML} > 2 = 2$ and $L_w/z_{AML} < -2 = -2$.

cooled (Figure 1). Initially winds were weak, air temperatures in the day exceeded lake temperatures, and a shallow diurnal thermocline (maximum buoyancy frequency N_{max} = 15 cycles per hour, cph), overlay the seasonal thermocline with N_{max} < 10 cph (Figure 1, 2–9 July). As the water column heated, z_{AML} became shallow (Figures 1b and 1e), and k_{600EC} had near zero values when winds were less than 2 m s^{-1}. Values at night, when z_{AML} increased with cooling and light winds, often exceeded 10 cm hr^{-1}. Air temperatures declined and wind speeds increased beginning on 10 July, and the diurnal thermocline deepened and merged with the seasonal thermocline (Figure 1e). The magnitude of k_{600EC} increased and decreased as winds similarly increased and decreased (Figures 1a and 1d). k_{600EC} reached 20–25 cm hr^{-1} when winds exceeded 6 m s^{-1}. Values were lower when winds were light and the lake was gaining heat. Exceptions to this pattern occurred. For instance, k_{600EC} exceeded 20 cm hr^{-1} near midnight when winds were light and the lake was losing heat (12 July). Computed ε during the period with higher winds ranged from 10^{-8} m^2 s^{-3} to 10^{-6} m^2 s^{-3} (Figure 2a) similar to observations in surface waters of other lakes [*MacIntyre et al.*, 1999] with the highest values during windy periods. Values of ε computed following *Lombardo and Gregg* [1989] from β alone ($u_* = 0$), ε_β, approached 10^{-7} m^2 s^{-3}. The dependence of k_{600EC} on turbulence in the upper water column is indicated by the concurrent increases and decreases in k_{600EC} and ε (Figures 2a and 2b). Similar patterns of change in k_{600SR} and in k_{600EC} provide evidence for the overall applicability of the surface renewal model (Figure 2b). In the following, we compare k_{600EC} and k_{600SR} for $\beta < 0$ and $\beta > 0$ to develop a mechanistic understanding of the processes affecting k_{600}.

3.2. Dependence of k_{600} on β

[8] Wind speeds prior to and during cooling influenced the magnitude of k_{600EC} (Figures 1d and 2b). During nocturnal cooling with the higher winds of 10 and 11 July, both k_{600SR} and k_{600EC} were elevated. $L_w/z_{AML} <= -1$ at those times, indicating wind stress dominated turbulence production in the actively mixing layer. However, during a lull when $L_w/ z_{AML} \rightarrow 0$, such that buoyancy dominated turbulence production in near surface waters, k_{600EC} stayed high and was higher than predicted based on ε. Surface currents or surface waves likely persisted and maintained the turbulence and resulting high values of k_{600EC}. On 13 July, $L_w/ z_{AML} <= -1$ during afternoon winds and k_{600EC} ranged from 15–25 cm hr^{-1}. As the wind decreased such that $L_w/ z_{AML} \rightarrow 0$, k_{600EC} was initially 15 cm hr^{-1} but dropped to values below 5 cm hr^{-1} by early morning 14 July. Again, it appeared that as the wind decreased, the turbulence

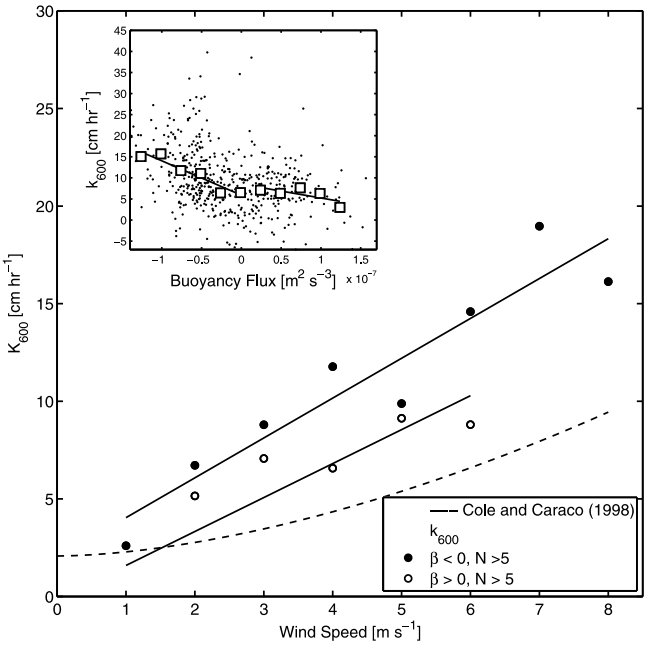

Figure 3. k_{600EC} versus U_{10} for buoyancy flux $\beta > 0$ (open circles) and $\beta < 0$ (closed circles). $k_{600\ EC}$ were averaged at 1 m s^{-1} intervals for bins with more than 5 data points. Insert. k_{600EC} versus β. Average values of $k_{600\ EC}$ for β and used in the regression binned at 0.25 × 10^{-7} m^2 s^{-3} intervals (boxes).

was initially sustained by residual currents or waves but as low winds persisted, the turbulence and k_{600EC} decreased such that k_{600EC} was similar to or slightly lower than k_{600SR} computed from ε_β, k_{600SR_β}. Values of k_{600EC} were of order 5 cm hr^{-1} during nocturnal cooling on 14–15 July when measured winds were light, and k_{600EC} was well approximated by k_{600SR_β}. These data indicate that the meteorological conditions at the time of measurement and the inertia within the lake determine the magnitude of turbulence and k_{600} when $\beta < 0$. When turbulence is induced by wind acting on the air-water interface ($L_w/z <= \sim -1$) or by preexisting currents, values of k_{600} are elevated. Values of k_{600} are lower when winds are light or remain light for some time. The close match between k_{600EC} and k_{600SR_β} early morning 13 and 14 July and late on 14 July and early morning 15 July suggests that k_{600} can be computed from β at such times.

[9] The response of k_{600EC} to changes in wind speed when the upper water column is heating, $\beta > 0$ and $L_w/z_{AML} > 0$, is variable. If winds were modest (4–7 m s^{-1}) at night and in the morning, k_{600EC} was in the range 10 to 15 cm hr^{-1} (Figure 2b; 11 July). When $U_{10} < 4$ m s^{-1} (Figure 2b; 11 and 15 July), and z_{AML} shallowed, k_{600EC} was less than predicted by k_{600SR} and often decreased below 5 cm hr^{-1}. The diminution, in contrast to observations when $\beta < 0$, indicates the wind induced turbulence was being damped by the heating and stratification. To quantify these effects, we follow *Brainerd and Gregg* [1993] and introduce a damping coefficient c_2/z_{AML} and compute dissipation as $\varepsilon = 0.84(0.58\beta + (c_2/z_{AML})(1.76u^3_{*w}/kz))$ when $L_w/z_{AML} >= 0$ and measured winds < 3 m s^{-1}. c_2 likely depends on the degree of stratification; the improvement in the match of k_{600SR} and k_{600EC} with $c_2 = 0.08$ on the afternoons of 11 and 15 July is illustrated in Figure 2b.

3.3. Regression Analyses

[10] The observations in 3.1 and 3.2 and the regressions in Figure 3 indicate that turbulence in the surface layer and k_{600} depend on wind speed and the heating or cooling of the upper water column. k_{600EC} was independent of β when the lake was heating ($\beta > 0$, $R^2 = 0.47$, p = 0.2), and negatively and significantly correlated to β when the lake was cooling ($\beta < 0$, $R^2 = 0.89$, p< 0.005) (Figure 3, insert, binned data). Regressions of k_{600EC} against U_{10} binned at intervals of 1 m s^{-1} are significant for $\beta > 0$ and $\beta < 0$ ($\beta < 0$, $k_{600} = 2.04$ (±0.35) $U_{10} + 2.0$ (±1.76), $R^2 = 0.88$, p < 0.001; $\beta > 0$, $k_{600} = 1.74$ (±0.63) $U_{10} - 0.15$ (±2.43), $R^2 = 0.76$, p = 0.024; all β, $k_{600} = 2.25$ (±0.33) $U_{10} + 0.16$ (±1.65), $R^2 = 0.91$, p < 0.001, standard errors in parentheses). The slopes of the lines are within the 95% confidence intervals for both cases and for the combined data. The intercept is higher for $\beta < 0$ than for $\beta > 0$ although not statistically distinct. However for $\beta < 0$, over 40% of the measurements of k_{600EC} exceeded 10 cm hr^{-1} whereas for $\beta > 0$, only 17% of the measurements were that high. Further, for $U_{10} < 1.5$ m s^{-1} and $\beta > 0$, average k_{600EC} was slightly negative indicating minimal or no flux. Based on this evidence, we infer that the greater intercept for $\beta < 0$ is meaningful. Values of k_{600EC} were higher than predicted using the regressions of *Cole and Caraco* [1998] (Figure 3). Our results are similar to those reported by *McGillis et al.* [2004], *Zappa et al.* [2007], and *Vachon et al.* [2010].

4. Discussion

[11] Quantifying the gas transfer coefficient in terms of the processes which induce turbulence at the air-water interface is an essential step for accurately estimating gas fluxes as needed in studies of lake metabolism and for regional and global carbon budgets. Here, for the first time in a stratified lake, we show how k_{600} varies with wind

forcing and buoyancy flux. Our approach involved modeling turbulence from surface meteorology to obtain estimates of the gas transfer coefficient which were then compared with estimates obtained from eddy covariance measurements. The overall successful match between k_{600EC} and k_{600SR} indicates that the turbulence at the air-water interface determines the gas transfer coefficient and that it can be computed using the surface renewal model. Our work confirms *Zappa et al.* [2007] who suggested that the surface renewal model is a general model which would apply in numerous aquatic ecosystems, but we extend the model by showing how conditions within the surface layer modify the turbulence and resulting k_{600} during light to moderate winds. Our regression analysis demonstrates that k_{600} is higher when lakes are cooling as opposed to heating.

[12] The analysis of the surface renewal model, as presented here, provides a framework for quantifying k_{600} as meteorological forcing of lakes varies by latitude, size, and degree of sheltering. Finding that k_{600} depends on β alone during cooling with light winds is particularly important for modeling fluxes from small lakes which are numerically dominant in the landscape but which tend to have low winds at night. The damping of turbulence during light to moderate winds with heating may vary with lake size and optical properties as larger lakes may sustain higher currents and larger waves and clearer lakes will heat and stratify less rapidly than more turbid ones. Systematic effort is required to quantify the time scales for set up and decay of currents and waves and for the damping of turbulence.

[13] In contrast to the wind-based models generally used to compute gas flux, this study provides separate regressions for k_{600} against wind for daytime when the water column heats and from late afternoon through early morning or on cloudy days when cooling occurs. Thereby flux estimates can be considerably improved. Equations such as these, which are based on variables that can be readily measured or modeled over large spatial scales, enable improved regional carbon budgets. The modeling will be improved further by consideration of co-occurring processes. Concentrations of greenhouse gases vary in surface waters due to biological activity and with the entrainment which accompanies nocturnal cooling, fall cooling, and storms [*Laurion et al.*, 2010; *Aberg et al.*, 2010]. The combination of increased greenhouse gases in surface waters during these events and higher gas transfer coefficients means that gas fluxes will vary non-linearly over diel cycles with further enhancement during storms. Thus, regional and global fluxes of greenhouse gases from lakes may be considerably larger than current estimates.

[14] **Acknowledgments.** Funding was provided by the U.S. National Science Foundation grants DEB0640953, DEB0919603, and ARC0714085 to SM, the Swedish Research Council, the Kempe, Ebba and Sven Schwarts, and Längman Foundations. Brian Emery, Craig Nelson, Thomas Westin and Ingemar Bergström provided technical support. The manuscript was improved by the critical comments of J. M. Melack, S. Sadro and two anonymous reviewers.

References

Aberg, J., M. Jansson, and A. Jonsson (2010), The importance of water temperature and thermal stratification dynamics for temporal variation of surface water CO_2 in a boreal lake, *J. Geophys. Res.*, *115*, G02024, doi:10.1029/2009JG001085.

Banerjee, S., and S. MacIntyre (2004), The air-water interface: Turbulence and scalar exchange, in Advances in *Coastal and Ocean Engineering*, vol. 9, edited by J. Grue et al., pp. 181–237, World Sci., Hackensack, N. J.

Brainerd, K. E., and M. C. Gregg (1993), Diurnal restratification and turbulence in the oceanic surface mixed layer: 2. Modeling, *J. Geophys. Res.*, *98*, 22,657–22,664, doi:10.1029/93JC02298.

Cole, J. J., and N. F. Caraco (1998), Atmospheric exchange of carbon dioxide in a low-wind oligotrophic lake measured by the addition of SF6, *Limnol. Oceanogr.*, *43*, 647–656, doi:10.4319/lo.1998.43.4.0647.

Cole, J. J., et al. (2007), Plumbing the global carbon cycle: Integrating inland waters into the terrestrial carbon budget, *Ecosystems*, *10*, 172–185, doi:10.1007/s10021-006-9013-8.

Crill, P. M., K. B. Bartlett, J. O. Wilson, D. I. Sebacher, R. C. Harriss, J. M. Melack, S. MacIntyre, L. Lesack, and L. Smith-Morrill (1988), Tropospheric methane from an Amazonian floodplain lake, *J. Geophys. Res.*, *93*, 1564–1570, doi:10.1029/JD093iD02p01564.

Imberger, J. (1985), The diurnal mixed layer, *Limnol. Oceanogr.*, *30*, 737–770, doi:10.4319/lo.1985.30.4.0737.

Jonsson, A., J. Aberg, A. Lindroth, and M. Jansson (2008), Gas transfer rate and CO_2 flux between an unproductive lake and the atmosphere in northern Sweden, *J. Geophys. Res.*, *113*, G04006, doi:10.1029/2008JG000688.

Laurion, I., W. F. Vincent, S. MacIntyre, L. Retamal, C. Dupont, P. Francus, and R. Pienitz (2010), Variability in greenhouse gas emissions from permafrost thaw ponds, *Limnol. Oceanogr.*, *55*, 115–133.

Lombardo, C. P., and M. C. Gregg (1989), Similarity scaling of viscous and thermal dissipation in a convective surface boundary layer, *J. Geophys. Res.*, *94*, 6273–6284, doi:10.1029/JC094iC05p06273.

MacIntyre, S., and J. M. Melack (2009), Mixing dynamics in lakes across climatic zones, in *Encyclopedia of Inland Waters*, edited by G. Likens, pp. 603–612, Elsevier, Oxford, U. K.

MacIntyre, S., R. Wanninkhof, and J. Chanton (1995), Trace gas exchange across the air-water interface in freshwater and coastal marine environments, in *Biogenic Trace Gases: Measuring Emissions From Soil and Water*, edited by P. Matson and R. Harriss, pp. 52–97, Blackwell, New York.

MacIntyre, S., W. Eugster, and G. W. Kling (2001), The critical importance of buoyancy flux for gas flux across the air-water interface, in *Gas Transfer at Water Surfaces*, edited by M. A. Donelan et al., pp. 135–139, AGU, Washington, D. C.

MacIntyre, S., J. R. Romero, and G. W. Kling (2002), Spatial-temporal variability in mixed layer deepening and lateral advection in an embayment of Lake Victoria, East Africa, *Limnol. Oceanogr.*, *47*, 656–671, doi:10.4319/lo.2002.47.3.0656.

MacIntyre, S., J. P. Fram, P. J. Kushner, N. D. Bettez, W. J. O'Brien, J. E. Hobbie, and G. W. Kling (2009), Climate-related variations in mixing dynamics in an Alaskan arctic lake, *Limnol. Oceanogr.*, *54*, 2401–2417.

MacIntyre, S., K. M. Flynn, R. Jellison, and J. R. Romero (1999), Boundary mixing and nutrient flux in Mono Lake, CA, *Limnol. Oceanogr.*, *44*, 512–529, doi:10.4319/lo.1999.44.3.0512.

McGillis, W. R., et al. (2004), Air-sea CO_2 exchange in the equatorial Pacific, *J. Geophys. Res.*, *109*, C08S02, doi:10.1029/2003JC002256.

Soloviev, A. V., and P. Schluessel (1994), Parameterization of the temperature difference across the cool skin of the ocean and the air-ocean gas transfer on the basis of modeling surface renewal, *J. Phys. Oceanogr.*, *24*, 1339–1346, doi:10.1175/1520-0485(1994)024<1339:POTCSO>2.0.CO;2.

Turney, D. E., and S. Banerjee (2008), Transport phenomena at interfaces between turbulent fluids, *AIChE J.*, *54*(2), 344–349, doi:10.1002/aic.11427.

Vachon, D., Y. T. Prairie, and J. J. Cole (2010), The relationship between near-surface turbulence and gas transfer velocity in freshwater systems and its implications for floating chamber measurements of gas exchange, *Limnol. Oceanogr.*, *55*, 1723–1732, doi:10.4319/lo.2010.55.4.1723.

Wanninkhof, R. H., W. E. Asher, D. T. Ho, C. Sweeney, and W. R. McGillis (2009), Advances in quantifying air-sea gas exchange and environmental forcing, *Annu. Rev. Mar. Sci.*, *1*, 213–244, doi:10.1146/annurev.marine.010908.163742.

Zappa, C. J., W. R. McGillis, P. A. Raymond, J. B. Edson, E. J. Hintsa, H. J. Zemmelink, J. W. H. Dacey, and D. T. Ho (2007), Environmental turbulent mixing controls on air-water gas exchange in marine and aquatic systems, *Geophys. Res. Lett.*, *34*, L10601, doi:10.1029/2006GL028790.

J. Aberg, M. Jansson, and A. Jonsson, Department of Ecology and Environmental Sciences, Umea University, SE-90187 Umea, Sweden.

S. MacIntyre, Department of Ecology, Evolution and Marine Biology, University of California, Santa Barbara, CA 93106, USA. (sally@icess.ucsb.edu)

S. D. Miller, Atmospheric Sciences Research Center, State University of New York at Albany, Albany, NY 12203, USA.

D. E. Turney, Earth Research Institute, University of California, Santa Barbara, CA 93106, USA.